THE JOURNAL OF PHYSICAL CHEMISTRY LETTERS
A JOURNAL OF THE AMERICAN CHEMICAL SOCIETY

pubs.acs.org/JPCL

Letter

One Ca^{2+} Site in CaNaY Zeolite Can Attach Three CO_2 Molecules

Nikola L. Drenchev, Elena Z. Ivanova, Mihail Y. Mihaylov, Hristiyan A. Aleksandrov, Georgi N. Vayssilov, and Konstantin I. Hadjiivanov*

Cite This: *J. Phys. Chem. Lett.* 2023, 14, 1564–1569

Read Online

ACCESS | Metrics & More | Article Recommendations | Supporting Information

ABSTRACT: To design efficient CO_2 capture materials, it is necessary to ensure a high adsorption capacity. We recently reported that one Na^+ site in NaY zeolite can attach two CO_2 molecules. However, the process is not suitable for practical use because it proceeds at a low temperature. Here, we present results on CO_2 adsorption on CaNaY zeolites, demonstrating that one Ca^{2+} site can attach three CO_2 molecules. The $\nu_3(^{13}CO_2)$ mode arising from the natural ^{13}C abundance allows for easy infrared monitoring of the processes: it appears at 2298, 2294, and 2291 cm^{-1} for the complexes with one, two, and three CO_2 ligands, respectively. The $^{12}CO_2$ molecules in the polyligand complexes interact vibrationally, leading to the split of the $\nu_3(^{12}CO_2)$ modes. At ambient temperature, $Ca^{2+}(CO_2)_2$ complexes predominate at >1 mbar CO_2 and triligand species begin to form at 65 mbar. The obtained results show that CaY zeolites can be very effective CO_2 capture materials.

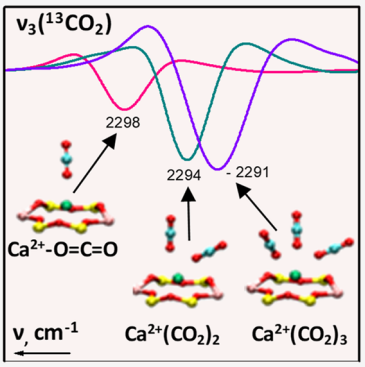

Global warming is one of the main current challenges facing modern society and is mainly caused by the increasing CO_2 concentration in the atmosphere.[1] Therefore, CO_2 capture is a very topical issue.[2,3] Adsorption processes are considered very promising for this purpose. To design efficient adsorbents, it is necessary to ensure both high adsorption capacity and suitable binding energy. Various approaches are currently being used by the scientific community,[2,3] and cation-exchanged zeolites have attracted much attention as potential CO_2 adsorbents.[4−27] An important feature of these materials is that, in many cases, large exchanged cations can simultaneously adsorb two[28−34] or even three small molecules as CO and N_2,[35−38] thus providing a high adsorption capacity. In a recent study,[27] we reported that, similar to CO and N_2, two CO_2 molecules can be simultaneously bound to one Na^+ cation in NaY. However, this occurs at a low temperature and is therefore of limited practical interest. The process can be optimized, for instance, by changing the nature of the exchanged cation. We concluded that one of the best candidates for this is Ca^{2+} for several reasons: (i) the ionic radius of Ca^{2+} is similar to that of Na^+, thus allowing for the formation of geminal complexes[34−37] but preventing the formation of M···O═C═O···M species;[14] (ii) the high electrophilicity of Ca^{2+} should ensure relatively strong adsorption of CO_2; and (iii) by analogy with CO, we hoped that up to three CO_2 molecules could coordinate to one Ca^{2+} site. Because the ν_3 frequency of adsorbed CO_2 depends upon the polarizing strength of the cation,[39] we also expected to spectrally distinguish adducts formed with Ca^{2+} and residual Na^+ sites.

Detailed information on experimental details, preparation of the samples, and basic sample characterization can be found in Figure S1 and the corresponding text of the Supporting Information.

Briefly, we studied two CaNaY samples differing in the Na/Ca ratio. They were prepared by ion-exchange using NaY (Si/Al = 2.6) as a starting material. Data on the chemical composition of the samples, according to energy-dispersive X-ray (EDX) analysis, are presented in Table 1. In the following, the samples with lower and higher Ca contents will be referred to as CaNaY(1) and CaNaY(2), respectively. The results presented here mainly consider the CaNaY(1) sample, because it allows for a better analysis of the very intense $\nu_3(^{12}CO_2)$ band. However, the conclusions drawn from the analysis of all spectral regions were essentially the same for both samples.

Table 1. Concentrations of Na and Ca in the Samples Studied

analysis results	CaNaY(1)	CaNaY(2)
atomic % Na	1.78	0.45
atomic % Ca	3.28	3.96
Na/Al atomic ratio	0.20	0.05
2Ca/Al atomic ratio	0.73	0.87

Received: October 31, 2022
Accepted: January 27, 2023
Published: February 6, 2023

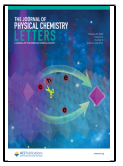

https://doi.org/10.1021/acs.jpclett.2c03294
J. Phys. Chem. Lett. 2023, 14, 1564−1569

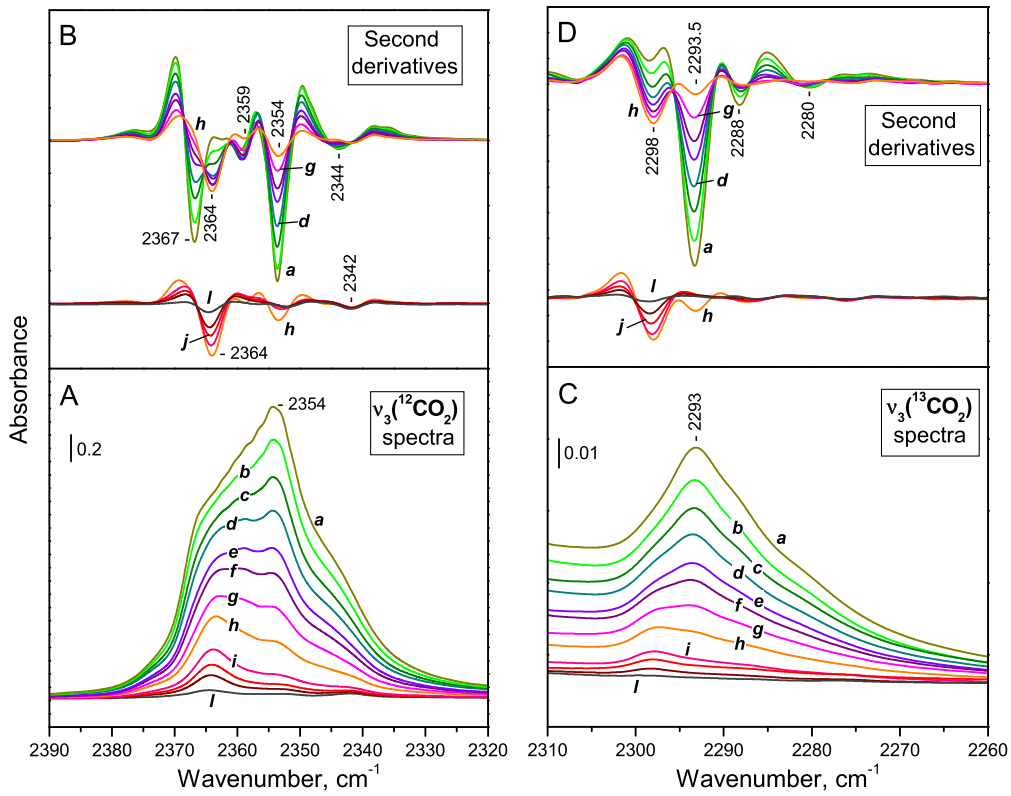

Figure 1. (A and C) FTIR spectra of CO_2 adsorbed on CaNaY(1) at ambient temperature. Equilibrium CO_2 pressure of (a) 6.8 mbar, (b) 5.8 mbar, (c) 4.0 mbar, (d) 3.0 mbar, (e) 2.2 mbar, (f) 1.7 mbar, (g) 1.0 mbar, and (h) 0.5 mbar and (i–l) development of spectra in dynamic vacuum. (B and D) Second derivatives of the spectra presented in panels A and C, respectively.

The Fourier transform infrared (FTIR) experiments were performed with self-supporting pellets activated in vacuum at 673 K. The FTIR spectra of CO_2 adsorbed on CaNaY(1) at ambient temperature and in the pressure range of 0–7 mbar are presented in panels A and C of Figure 1. In the $\nu_3(^{12}CO_2)$ region (Figure 1A), a band at 2364 cm^{-1} is formed at low coverage and attributed to $Ca^{2+}\cdots O{=}C{=}O$ adducts.[10,11] Note that the highest frequency ν_3 band, observed after CO_2 adsorption on NaY, is at 2354 cm^{-1}.[13−21] As the coverage increases, the band initially develops and then a complex feature is formed in the 2380–2330 cm^{-1} region.

As a result of the natural abundance of ^{13}C (ca. 1.1%), it is also possible to follow the spectra in the $\nu_3(^{13}CO_2)$ region (Figure 1C). At low coverage, the ν_3 band of $Ca^{2+}\cdots O{=}^{13}C{=}O$ species is detected at 2298 cm^{-1}. With increasing coverage, mainly a broad band centered at 2293 cm^{-1} develops. The isotopic shift factor (1.029) coincides with the reported value.[40] Even a cursory glance shows that the spectra in the $\nu_3(^{12}CO_2)$ and $\nu_3(^{13}CO_2)$ regions look differently. This indicates that some vibrational interaction occurs between the adsorbed $^{12}CO_2$ molecules. This interaction is not registered with the $^{13}CO_2$ molecules because they are too diluted to interact with each other.

For more precise analysis of the spectra, we used the second derivatives. We start the discussion with the spectra in the $^{13}CO_2$ region because they are simpler (Figure 1D). The results allow for the conclusion of the existence of two main stages of the spectra evolution. First, with the coverage increase, the band at 2298 cm^{-1} appears and rises in intensity (lower set of spectra). At the end of this stage, a weak band at 2293.5 cm^{-1} also appears.

During the second stage, the band at 2298 cm^{-1} declines and the band at 2293.5 cm^{-1} develops at its expense. A well-defined isosbestic point indicates direct conversion of one species into another. At high coverage, signals associated with the presence of residual Na^+ cations also appear. A band at 2288 cm^{-1} is assigned to $Na^+\cdots O{=}^{13}C{=}O$ adducts, and a weak band at 2280 cm^{-1} is assigned to a small amount of $Na^+(O{=}^{12}C{=}O)(O{=}^{13}C{=}O)$ geminal species.[27] Indeed, these bands appear with reduced intensity with the CaNaY(2) sample having a lower sodium content.

The band at 2298 cm^{-1}, registered at low coverage, was already assigned to the $\nu_3(^{13}CO_2)$ mode of $Ca^{2+}\cdots O{=}^{13}C{=}O$ adducts. Consequently, the band at 2293.5 cm^{-1} is attributed to the $\nu_3(^{13}CO_2)$ mode of $Ca^{2+}(O{=}^{12}C{=}O)(O{=}^{13}C{=}O)$ geminal species. Note that, as a result of the low concentration of $^{13}CO_2$, $Ca^{2+}(^{13}CO_2)_2$ complexes are practically absent.

Consider now the $\nu_3(^{12}CO_2)$ region (Figure 1B). At low coverage, mainly the $Ca^{2+}\cdots O{=}^{12}C{=}O$ band at 2364 cm^{-1} develops. With a further coverage increase, this band declines and two bands develop at 2367 and 2354 cm^{-1}. In addition, weaker bands at 2359 and 2344 cm^{-1} are formed. The band at 2344 cm^{-1} corresponds to the $^{13}CO_2$ band at 2280 cm^{-1} and is associated with species formed with Na^+ sites.[27] The same accounts for a part of the band at 2354 cm^{-1} (respective $^{13}CO_2$ band at 2288 cm^{-1}) However, a comparison to the spectra in the $^{13}CO_2$ region shows that the band is much more intense than its $^{13}CO_2$ analogue, which indicates that the main part of the band is due to species formed with Ca^{2+} sites. The band at 2359 cm^{-1} corresponds to the band at 2293.5 cm^{-1} in the $^{13}CO_2$ region and can be associated with mixed ligand

https://doi.org/10.1021/acs.jpclett.2c03294
J. Phys. Chem. Lett. 2023, 14, 1564−1569

complexes, $Ca^{2+}(O{=}{}^{12}C{=}O)(O{=}{}^{13}C{=}O)$. However, the contribution of other species to this band is not excluded.

The bands at 2367 and 2354 cm^{-1} develop almost in parallel and are associated with geminal $Ca^{2+}(^{12}CO_2)_2$ adducts. Therefore, the $\nu_3(^{12}CO_2)$ mode splits into two components. We attribute them to the in-phase and out-of-phase ν_3 modes of geminal $Ca^{2+}(^{12}CO_2)_2$ complexes, respectively.

To verify the possibility of the simultaneous coordination of three CO_2 molecules to one Ca^{2+} cation, we performed variable temperature infrared (VTIR) experiments. Initially, CO_2 was adsorbed at 2.6 mbar equilibrium pressure, and then the temperature was gradually lowered to shift the equilibrium toward adsorbed species. The $\nu_3(^{12}CO_2)$ band was too intense to be followed accurately. Selected spectra in the $\nu_3(^{13}CO_2)$ region are presented in Figure 2. Here again, we detected different stages of the process.

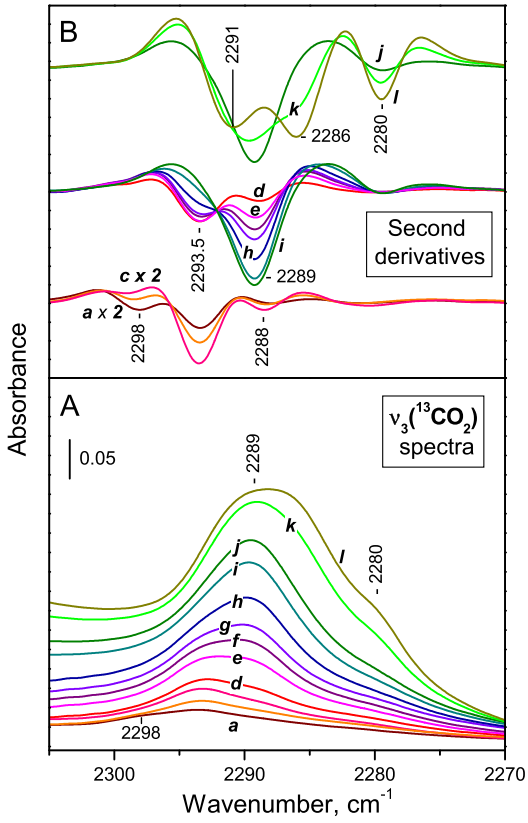

Figure 2. (A) VTIR spectra in the $\nu_3(^{13}CO_2)$ region of CO_2 (2.6 mbar initial equilibrium pressure) adsorbed on CaNaY(1). Sample temperature of (a) 293 K, (b) 257 K, (c) 240 K, (d) 224 K, (e) 215 K, (f) 211 K, (g) 205 K, (h) 199 K, (i) 190 K, (j) 184 K, (k) 177 K, and (l) 171 K. The spectra are background- and gas-phase-corrected. (B) Second derivative of the spectra presented in panel A.

The first stage (Figure 2B, lowest set) is identical to the already described conversion of $Ca^{2+}(^{13}CO_2)$ to $Ca^{2+}(^{12}CO_2)$-$(^{13}CO_2)$ adducts. During the second stage (Figure 2B, middle set), the band characterizing diligand species (2293.5 cm^{-1}) decreases in intensity to ultimately disappear and a new, more intense band at 2289 cm^{-1} develops at its expense. These results clearly demonstrate conversion of the $Ca^{2+}(^{12}CO_2)$-$(^{13}CO_2)$ adducts into other species absorbing around 2289 cm^{-1}. In this case again, an isosbestic point indicates conversion of one species into another. Therefore, we assign the band at 2289 cm^{-1} to triligand $Ca^{2+}(^{12}CO_2)_2(^{13}CO_2)$ species.

It should be noted that the band at 2289 cm^{-1} is a composite, because under the conditions applied, $Na^+\cdots O{=}{}^{13}C{=}O$ adducts absorbing at 2288 cm^{-1} are also formed.[27] This is confirmed by the spectra registered at a further coverage increase (Figure 2B, top set), where part of the 2289 cm^{-1} band arising from $Na^+\cdots O{=}{}^{13}C{=}O$ adducts is converted into other species (band at 2286 cm^{-1} as a result of the change of the molecule orientation and band at 2280 cm^{-1} as a result of geminal CO_2 species on Na^+ sites).[27] Simultaneously, the triligand $Ca^{2+}(^{12}CO_2)_2(^{13}CO_2)$ species are clearly visible by a separate band at 2291 cm^{-1}.

Here, we want to highlight the remarkable similarity between the spectra presented in Figure 2B and the spectra of CO adsorbed at a low temperature on CaNaY(1) (Figure S2 of the Supporting Information), which confirms our conclusions.

As a result of the high intensity of the $\nu_3(^{12}CO_2)$ bands, we cannot draw firm conclusions on the spectral performance of the $Ca^{2+}(^{12}CO_2)_3$ species in the region. However, we detected, by the second derivatives, a band at 2372 cm^{-1} that is distant from the main maximum. The results are presented in Figure S3 of the Supporting Information. On the basis of this finding, we analyzed the second derivatives of a set of spectra recorded at ambient temperature and high CO_2 equilibrium pressures (up to 200 mbar). The band at 2372 cm^{-1} was found to appear at about 65 mbar (see Figure S3 of the Supporting Information); i.e., at this pressure, $Ca^{2+}(^{12}CO_2)_3$ species are already formed.

We also detected, albeit with very low intensity, the ν_1 and $2\nu_2$ modes of adsorbed CO_2, which are normally infrared (IR) silent. Their intensity is higher with the CaNaY(2) sample. Briefly, the maximum of the ν_1 band appears at 1378 cm^{-1} and is hardly sensitive to the formation of di- and triligand species (Figure S4 of the Supporting Information). In contrast, the $2\nu_2$ band appears at 1269 cm^{-1} and splits into two components, at 1274 and 1268 cm^{-1}, for the diligand species. The spectra of the $Ca^{2+}(CO_2)_3$ species are similar; i.e., the $2\nu_2$ mode is not active for the third adsorbed molecule. For both bands (ν_1 and $2\nu_2$), the extinction coefficient decreases with an increasing number of CO_2 molecules attached to one site.

To estimate the amount of CO_2 adsorbed on cationic sites, we performed experiments on successive adsorption of small doses of CO_2 on the CaNaY(2) sample at 223 K. The spectra in the $\nu_3(^{13}CO_2)$ region are presented in Figure 3A and are consistent with the conclusions already drawn. In this case, the band at 2280 cm^{-1}, associated with the presence of Na^+, appears with reduced intensity, and the band indicative of triligand species is detected at 2291.5 cm^{-1}.

As a result of the higher calcium content, we also clearly detected the $(\nu_1 + \nu_3)(^{12}CO_2)$ combination bands (Figure 3B). The mono-, di-, and triligand species are observed at 3721, 3715.5, and 3713 cm^{-1}, respectively. This mode is convenient for quantification because the baseline is flat. The dependence of the integral absorbance upon the amount of CO_2 added is a straight line for the first doses (see the inset in Figure 3B). Assuming the same extinction coefficient for the bands in the 3725−3710 cm^{-1} region, we estimated that the maximal amount of CO_2 adsorbed on cationic sites is 7.23 wt %. The intensity of the $\nu_3(^{13}CO_2)$ band also depends linearly upon the amount of CO_2 added to the system for the first doses. However, at higher coverage, the complex baseline affects

https://doi.org/10.1021/acs.jpclett.2c03294
J. Phys. Chem. Lett. 2023, 14, 1564−1569

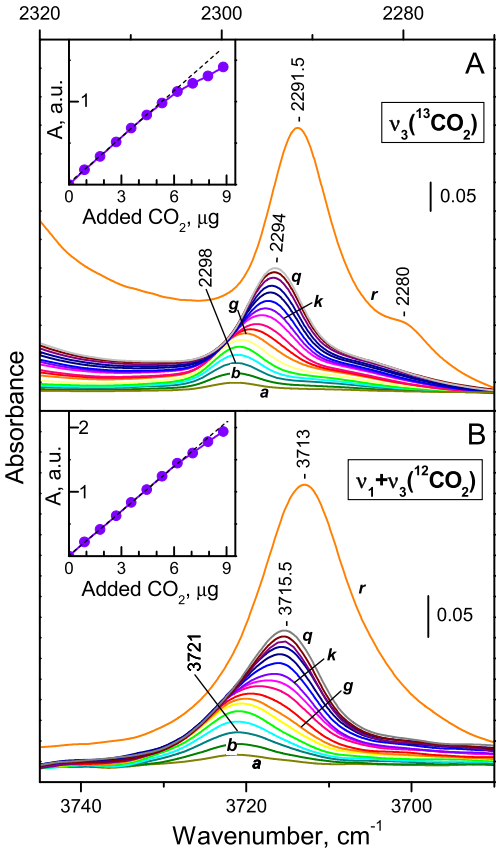

Figure 3. FTIR spectra registered after successive dosing of CO_2 on the CaNaY(2) sample (a−q) at 223 K and (r) under 7 mbar equilibrium CO_2 pressure. (A) $\nu_3(^{13}CO_2)$ region. (B) $\nu_1 + \nu_3(^{12}CO_2)$ region. The insets show the dependence of the integral absorbance of the respective bands on the amount of CO_2 added to the system. The pellet weight was 20 mg.

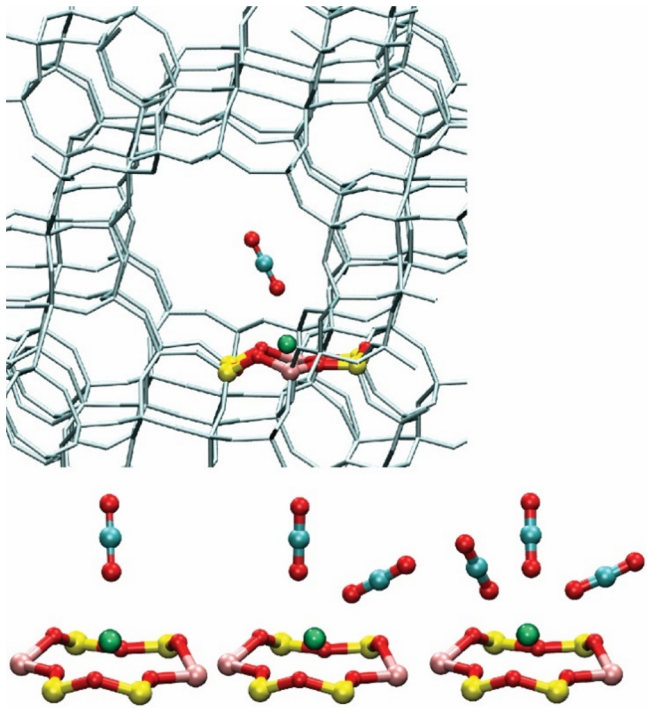

Figure 4. Optimized structures of the complexes of Ca^{2+} in the S_{II} position in FAU zeolite (model with Si/Al = 95) with one, two, and three CO_2 ligands: location of the complex in the zeolite cavity and close views of the three complexes. Colors: red, oxygen; yellow, silicon; pink, aluminum; blue, carbon; and green, calcium.

accurate integration. Nevertheless, the spectra in the $\nu_3(^{13}CO_2)$ region allowed us to estimate the contribution of the Na^+ sites (band at 2280 cm^{-1}) to the CO_2 adsorption uptake to be 10.2%. Thus, the amount of CO_2 adsorbed on Ca^{2+} sites appears to be 6.49 wt %.

It is known that in dehydrated Y zeolite Na^+ and Ca^{2+} cations occupy different positions (S_I, S_I', and S_{II}).[41] Among these, only cations in S_{II} positions are accessible to adsorption.[39] Thus, the results are consistent with the idea that more than one CO_2 molecule binds to a single Ca^{2+} site in S_{II} position. These results are also in agreement with the adsorption isotherms, showing that CO_2 uptake at 277 K and 350 mbar pressure is 7.6 wt % (see Figure S5 of the Supporting Information).

We also complemented the experimental observations with computational modeling using periodic density functional calculations for models of the FAU structure with Si/Al = 95 and 2.49, respectively. The optimized structures of the complexes are shown in Figure 4. The binding energy of the complex with one CO_2 molecule in the low-silica model, Si/Al = 2.49, is −50 kJ mol^{-1}, while the value per adsorbed CO_2 in the complexes with two and three ligands is lower, −48 and −40 kJ mol^{-1}, respectively. The calculated Gibbs free energies at 173 K are −1, 1, and 9 kJ mol^{-1} for the complexes with one, two, and three ligands, respectively (see Table S1 of the Supporting Information) as a result of entropy loss upon adsorption of the gas molecules. Although the binding energy per ligand in the complexes is similar, the two- and three-ligand complexes are observed at higher pressure likely as a result of the presence of many cations in zeolite cavity and repulsion between ligands adsorbed at those cations. The stability of the complexes with one, two, and three ligands in the high-silica model, Si/A l= 95, are similar, at −61, −47, and −46 kJ mol^{-1}, respectively (Table S1 of the Supporting Information). The non-specific interaction of CO_2 with the zeolite wall in the region far from the metal cation is −18 kJ mol^{-1}, which coincides with the contribution of the dispersion interaction in the binding energy per ligand in the modeled complexes, from −19 to −16 kJ mol^{-1}. Thus, the contribution of the electrostatic interactions between the ligand and the calcium cation is 60−70% of the binding energy.

We also calculated the vibrational frequencies of adsorbed CO_2. The calculated values are corrected by −16 cm^{-1}, which is the difference between experimental and calculated values for CO_2 in the gas phase, 2365 and 2349 cm^{-1}, respectively[42] (Table S1 of the Supporting Information). The calculated frequencies of the complexes with one and two ligands in the low-silica model, 2371 and 2375/2365 cm^{-1}, respectively, fit very well to the corresponding experimental values, 2364 and 2367/2354 cm^{-1}. Changes in the vibrational frequencies in the mixed complexes with $^{12}CO_2$ and $^{13}CO_2$, observed experimentally are also well-reproduced. As expected, for the $Ca^{2+}(^{12}CO_2)_3$ complex, the calculations result in three vibrational frequencies, at 2377, 2365, and 2353 cm^{-1}. However, only the highest frequency band was experimentally observed because the other bands were masked by the other strong bands in the region. Despite different aluminum contents in the high-silica model, the calculated vibrational frequencies of CO_2 in the complexes with one, two, or three

https://doi.org/10.1021/acs.jpclett.2c03294
J. Phys. Chem. Lett. 2023, 14, 1564−1569

ligands differ by only 7 cm^{-1} from those in the high-silica model (Table S1 of the Supporting Information). Thus, they also fit well to the experimental values.

Finally, we emphasize that CaY zeolites possess a high CO_2 adsorption capacity at ambient temperature. Each Ca^{2+} site can attach two CO_2 molecules at relatively low partial pressure and has the reserve potential to bind an additional molecule when the equilibrium pressure increases. In contrast, at ambient temperature, each Na^+ site in NaY can attach only one CO_2 molecule and the adsorption enthalpy is low, which results in poor adsorption capacity at a relatively low CO_2 partial pressure. We believe that the results reported in this study will contribute to the development of CaY-based adsorbents for CO_2 having high adsorption capacity.

■ ASSOCIATED CONTENT

Supporting Information

The Supporting Information is available free of charge at https://pubs.acs.org/doi/10.1021/acs.jpclett.2c03294.

Experimental details, background spectra, spectra in the regions of the ν_1 and $2\nu_2$ modes, spectra of low-temperature CO adsorption, second derivatives of spectra at low and ambient temperatures, and experimental and calculated frequencies of adsorbed CO_2 (PDF)

■ AUTHOR INFORMATION

Corresponding Author

Konstantin I. Hadjiivanov − *Institute of General and Inorganic Chemistry, Bulgarian Academy of Sciences, 1113 Sofia, Bulgaria;* orcid.org/0000-0002-7622-4620; Email: kih@svr.igic.bas.bg

Authors

Nikola L. Drenchev − *Institute of General and Inorganic Chemistry, Bulgarian Academy of Sciences, 1113 Sofia, Bulgaria*

Elena Z. Ivanova − *Institute of General and Inorganic Chemistry, Bulgarian Academy of Sciences, 1113 Sofia, Bulgaria*

Mihail Y. Mihaylov − *Institute of General and Inorganic Chemistry, Bulgarian Academy of Sciences, 1113 Sofia, Bulgaria;* orcid.org/0000-0001-5084-0452

Hristiyan A. Aleksandrov − *Institute of General and Inorganic Chemistry, Bulgarian Academy of Sciences, 1113 Sofia, Bulgaria; Faculty of Chemistry and Pharmacy, University of Sofia, 1126 Sofia, Bulgaria;* orcid.org/0000-0001-8311-5193

Georgi N. Vayssilov − *Faculty of Chemistry and Pharmacy, University of Sofia, 1126 Sofia, Bulgaria;* orcid.org/0000-0002-5185-8002

Complete contact information is available at: https://pubs.acs.org/10.1021/acs.jpclett.2c03294

Notes

The authors declare no competing financial interest.

■ ACKNOWLEDGMENTS

The experimental part of the work was supported by the National Science Fund of Bulgaria, Contract KP-06-DV/1, from 2021. Thanks are due to Discoverer PetaSC and EuroHPC JU for awarding access to Discoverer supercomputer resources.

■ REFERENCES

(1) Al-Ghussain, L. Global Warming: Review on Driving Forces and Mitigation. *AIChE J.* **2019**, *38*, 13−21.

(2) Gür, T. M. Carbon Dioxide Emissions, Capture, Storage and Utilization: Review of Materials, Processes and Technologies. *Prog. Energy Combust. Sci.* **2022**, *89*, 100965.

(3) Baena-Moreno, F. M.; Rodríguez-Galán, M.; Vega, F.; Alonso-Fariñas, B.; Vilches Arenas, L. F.; Navarrete, B. Carbon Capture and Utilization Technologies: A Literature Review and Recent Advances. *Energy Sources, Part A* **2019**, *41*, 1403−1433.

(4) Kumar, S.; Srivastava, R.; Koh, J. Utilization of Zeolites as CO_2 Capturing Agents: Advances and Future Perspectives. *J. CO2 Util.* **2020**, *41*, 101251.

(5) de Aquino, T. F.; Estevam, S. T.; Viola, V. O.; Marques, C. R. M.; Zancan, F. L.; Vasconcelos, L. B.; Riella, H. G.; Pires, M. J. R.; Morales-Ospino, R.; Torres, A. E. B.; Bastos-Neto, M.; Cavalcante, C. L., Jr. CO_2 Adsorption Capacity of Zeolites Synthesized from Coal Fly Ashes. *Fuel* **2020**, *276*, 118143.

(6) Dabbawala, A. A.; Ismail, I.; Vaithilingam, B. V.; Polychronopoulou, K.; Singaravel, G.; Morin, S.; Berthod, M.; Al Wahedi, Y. Synthesis of Hierarchical Porous Zeolite-Y for Enhanced CO_2 Capture. *Microporous Mesoporous Mater.* **2020**, *303*, 110261.

(7) Boycheva, S.; Chakarova, K.; Mihaylov, M.; Hadjiivanov, C.; Popova, M. Effect of Calcium on Enhanced Carbon Capture Potential of Coal Fly Ash Zeolites. Part II: A Study on the Adsorption Mechanisms. *Environ. Sci.: Processes Impacts* **2022**, *24*, 1934−1944.

(8) Xu, M.; Chen, S.; Seo, D.-K.; Deng, S. Evaluation and Optimization of VPSA Processes with Nanostructured Zeolite NaX for Post-combustion CO_2 Capture. *Chem. Eng. J.* **2019**, *371*, 693−705.

(9) Liu, L.; Du, T.; Li, G.; Yang, F.; Che, S. Using one Waste to Tackle Another: Preparation of a CO_2 Capture Material Zeolite X from Laterite Residue and Bauxite. *J. Hazard. Mater.* **2014**, *278*, 551−558.

(10) Montanari, T.; Busca, G. On the Mechanism of Adsorption and Separation of CO_2 on LTA Zeolites: An IR Investigation. *Vibr. Spectrosc.* **2008**, *46*, 45−51.

(11) Jacobs, P. A.; van Cauwelaert, F. H.; Vansant, E. F.; Uytterhoeven, J. B. Surface Probing of Synthetic Faujasites by Adsorption of Carbon Dioxide. Part I. Infra-red Study of Carbon Dioxide Adsorbed on Na-Ca-Y and Na-Mg-Y Zeolites. *J. Chem. Soc., Faraday Trans. 1* **1973**, *69*, 1056−1068.

(12) Villarreal, A.; Garbarino, G.; Riani, P.; Finocchio, E.; Bosio, B.; Ramírez, J.; Busca, G. Adsorption and Separation of CO_2 from N_2-rich Gas on Zeolites: Na-X Faujasite vs Na-mordenite. *J. CO2 Util.* **2017**, *19*, 266−275.

(13) Bekhti, H.; Boucheffa, Y.; Ait Blal, A. H.; Travert, A. In Situ FTIR Investigation of CO_2 Adsorption over MgO-impregnated NaY Zeolites. *Vibr. Spectrosc.* **2021**, *117*, 103313.

(14) Thang, H. V.; Grajciar, L.; Nachtigall, P.; Bludsky, O.; Areán, C. O.; Frydová, E.; Bulánek, R. Adsorption of CO_2 in FAU Zeolites: Effect of Zeolite Composition. *Catal. Today* **2014**, *227*, 50−56.

(15) Pirngruber, G. D.; Raybaud, P.; Belmabkhout, Y.; Cejka, J.; Zukal, A. The Role of the Extra-framework Cations in the Adsorption of CO_2 on Faujasite Y. *Phys. Chem. Chem. Phys.* **2010**, *12*, 13534−13546.

(16) Galhotra, P.; Navea, J. G.; Larsen, S. C.; Grassian, V. H. Carbon dioxide ($C^{16}O_2$ and $C^{18}O_2$) Adsorption in Zeolite Y Materials: Effect of Cation, Adsorbed Water and Particle Size. *Energy Environ. Sci.* **2009**, *2*, 401−409.

(17) Polisi, M.; Grand, J.; Arletti, R.; Barrier, N.; Komaty, S.; Zaarour, M.; Mintova, S.; Vezzalini, G. CO_2 Adsorption/Desorption in FAU Zeolite Nanocrystals: In Situ Synchrotron X-ray Powder Diffraction and In Situ Fourier Transform Infrared Spectroscopic Study. *J. Phys. Chem. C* **2019**, *123*, 2361−2369.

(18) Martra, G.; Coluccia, S.; Davit, P.; Gianotti, E.; Marchese, L.; Tsuji, H.; Hattori, H. Acidic and Basic Sites in NaX and NaY

Faujasites Investigated by NH_3, CO_2 and CO Molecular Probes. *Res. Chem. Intermed.* **1999**, *25*, 77−93.
(19) Plant, D. F.; Maurin, G.; Jobic, H.; Llewellyn, P. L. Molecular Dynamics Simulation of the Cation Motion upon Adsorption of CO_2 in Faujasite Zeolite Systems. *J. Phys. Chem. B* **2006**, *110*, 14372−14378.
(20) Plant, D. F.; Maurin, G.; Deroche, I.; Llewellyn, P. L. Investigation of CO_2 Adsorption in Faujasite Systems: Grand Canonical Monte Carlo and Molecular Dynamics Simulations Based on a New Derived Na^+-CO_2 Force Field. *Microporous Mesoporous Mater.* **2007**, *99*, 70−78.
(21) Yang, K.; Yang, G.; Wu, J. Quantitatively Understanding the Insights into CO_2 Adsorption on Faujasite from the Heterogeneity and Occupancy Sequence of Adsorption Sites. *J. Phys. Chem. C* **2021**, *125*, 15676−15686.
(22) Bonelli, B.; Civalleri, B.; Fubini, B.; Ugliengo, P.; Areán, C. O.; Garrone, E. Experimental and Quantum Chemical Studies on the Adsorption of Carbon Dioxide on Alkali-Metal-Exchanged ZSM-5 Zeolites. *J. Phys. Chem. B* **2000**, *104*, 10978−10988.
(23) Bonelli, B.; Onida, B.; Fubini, B.; Areán, C. O.; Garrone, E. Vibrational and Thermodynamic Study of the Adsorption of Carbon Dioxide on the Zeolite Na-ZSM-5. *Langmuir* **2000**, *16*, 4976−4983.
(24) Bulanek, R.; Frolich, K.; Frydova, E.; Cicmanec, P. Microcalorimetric and FTIR Study of the Adsorption of Carbon Dioxide on Alkali-metal Exchanged FER Zeolites. *Top. Catal.* **2010**, *53*, 1349−1360.
(25) Montanari, T.; Finocchio, E.; Salvatore, E.; Garuti, G.; Giordano, A.; Pistarino, C.; Busca, G. CO_2 Separation and Landfill Biogas Upgrading: A Comparison of 4A and 13X Zeolite Adsorbents. *Energy* **2011**, *36*, 314−319.
(26) Ohlin, L.; Bazin, P.; Thibault-Starzyk, F.; Hedlund, J.; Grahn, M. Adsorption of CO_2, CH_4, and H_2O in Zeolite ZSM-5 Studied Using In Situ ATR-FTIR Spectroscopy. *J. Phys. Chem. C* **2013**, *117*, 16972−16982.
(27) Chakarova, K.; Mihaylov, M.; Hadjiivanov, K. Can Two CO_2 Molecules Be Simultaneously Bound to One Na^+ Site in NaY Zeolite? A Ddetailed FTIR Investigation. *Microporous Mesoporous Mater.* **2022**, *345*, 112270.
(28) Hadjiivanov, K.; Knözinger, H. FTIR Spectroscopic Evidence of Formation of Geminal Dinitrogen Species during the Low-temperature N_2 Adsorption on NaY Zeolites. *Catal. Lett.* **1999**, *58*, 21−26.
(29) Hadjiivanov, K.; Knözinger, H. FTIR Study of the Low-temperature Adsorption and Co-adsorption of CO and N_2 on NaY Zeolite: Evidence of Simultaneous Coordination of Two Molecules to One Na^+ site. *Chem. Phys. Lett.* **1999**, *303*, 513−520.
(30) Nour, Z.; Berthomieu, D. Multiple Adsorption of CO on Na-exchanged Y Faujasite: A DFT Investigation. *Mol. Simul.* **2014**, *40*, 33−44.
(31) Hadjiivanov, K.; Massiani, P.; Knözinger, H. Low Temperature CO and $^{15}N_2$ Adsorption and Co-adsorption on Alkali Cation Exchanged EMT Zeolites: An FTIR Study. *Phys. Chem. Chem. Phys.* **1999**, *1*, 3831−3838.
(32) Zecchina, A.; Otero Areán, C.; Turnes Palomino, G.; Geobaldo, F.; Lamberti, C.; Spoto, G.; Bordiga, S. The Vibrational Spectroscopy of H_2, N_2, CO and NO Adsorbed on the Titanosilicate Molecular Sieve ETS-10. *Phys. Chem. Chem. Phys.* **1999**, *1*, 1649−1657.
(33) Hadjiivanov, K.; Ivanova, E.; Kantcheva, M.; Ciftlikli, E. Z.; Klissurski, D.; Dimitrov, L.; Knözinger, H. FTIR Study of Low-temperature CO Adsorption on Mn-ZSM-5 and MnY Zeolites. Effect of the Zeolite Matrix on the Formation of $Mn^{2+}(CO)_2$ Geminal Species. *Catal. Commun.* **2002**, *3*, 313−319.
(34) Paukshtis, E.; Soltanov, R.; Yurchenko, E. IR Spectroscopic Studies of Low-temperature CO Adsorption on CaNaY Zeolite. *React. Kinet. Catal. Lett.* **1983**, *22*, 147−151.
(35) Hadjiivanov, K.; Knözinger, H. Formation of $Ca^{2+}(CO)_3$ Complexes during Low-Temperature CO Adsorption on CaNaY Zeolite. *J. Phys. Chem. B* **2001**, *105*, 4531−4534.
(36) Hadjiivanov, K.; Knözinger, H.; Ivanova, E.; Dimitrov, L. FTIR Study of Low-temperature CO and $^{15}N_2$ Adsorption on a CaNaY Zeolite: Formation of Site-specified $Ca^{2+}(CO)_3$ and $Ca^{2+}(^{15}N_2)_3$ Complexes. *Phys. Chem. Chem. Phys.* **2001**, *3*, 2531−2536.
(37) Hadjiivanov, K.; Ivanova, E.; Knözinger, H. FTIR Study of Low-temperature CO Adsorption on Y Zeolite Exchanged with Be^{2+}, Mg^{2+}, Ca^{2+}, Sr^{2+} and Ba^{2+} Cations. *Microporous Mesoporous Mater.* **2003**, *58*, 225−236.
(38) Lamberti, C.; Bordiga, S.; Salvalaggio, M.; Spoto, G.; Zecchina, A.; Geobaldo, F.; Vlaic, G.; Bellatreccia, M. XAFS, IR, and UV-Vis Study of the Cu^I Environment in Cu^I-ZSM-5. *J. Phys. Chem. B* **1997**, *101*, 344−360.
(39) Knözinger, H.; Huber, S. IR Spectroscopy of Small and Weakly Interacting Molecular Probes for Acidic and Basic Zeolites. *J. Chem. Soc., Faraday Trans.* **1998**, *94*, 2047−2059.
(40) Pinchas, S.; Laulicht, I. *Infrared Spectra of Labelled Compounds*; Academic Press, London, U.K., 1971.
(41) Frising, T.; Leflaive, P. Extraframework Cation Distributions in X and Y Faujasite Zeolites: A Review. *Microporous Mesoporous Mater.* **2008**, *114*, 27−63.
(42) Shimanouchi, T. *Tables of Molecular Vibrational Frequencies Consolidated*; National Bureau of Standards (NBS): Gaithersburg, MD, 1972; Vol. *1*, pp 1−160.

https://doi.org/10.1021/acs.jpclett.2c03294
J. Phys. Chem. Lett. 2023, 14, 1564−1569